The global distribution of cultivable lands: current patterns and sensitivity to possible climate change

Article · January 2002

CITATIONS
229

READS
311

4 authors, including:

Navin Ramankutty
University of British Columbia - Vancouver
180 PUBLICATIONS **23,124** CITATIONS
SEE PROFILE

John Norman
University of Wisconsin–Madison
282 PUBLICATIONS **19,748** CITATIONS
SEE PROFILE

Kevin Mcsweeney
University of Wisconsin–Madison
51 PUBLICATIONS **1,417** CITATIONS
SEE PROFILE

Global Ecology & Biogeography (2002) **11**, 377–392

RESEARCH ARTICLE

The global distribution of cultivable lands: current patterns and sensitivity to possible climate change

NAVIN RAMANKUTTY*, JONATHAN A. FOLEY*, JOHN NORMAN*† and KEVIN MCSWEENEY†

**Center for Sustainability and the Global Environment (SAGE), Gaylord Institute for Environmental Studies, University of Wisconsin, 1710 University Avenue, Nelson, Madison, Wisconsin, 53726, U.S.A. †Department of Soil Science, University of Wisconsin, 1525 Observatory Drive, Madison, Wisconsin, 53706, U.S.A.*

ABSTRACT

Aim This study makes quantitative global estimates of land suitability for cultivation based on climate and soil constraints. It evaluates further the sensitivity of croplands to any possible changes in climate and atmospheric CO_2 concentrations.

Location The location is global, geographically explicit.

Methods The methods used are spatial data synthesis and analysis and numerical modelling.

Results There is a cropland 'reserve' of 120%, mainly in tropical South America and Africa. Our climate sensitivity analysis indicates that the southern provinces of Canada, north-western and north-central states of the United States, northern Europe, southern Former Soviet Union and the Manchurian plains of China are most sensitive to changes in temperature. The Great Plains region of the United States and north-eastern China are most sensitive to changes in precipitation. The regions that are sensitive to precipitation change are also sensitive to changes in CO_2, but the magnitude is small compared to the influence of direct climate change. We estimate that climate change, as simulated by global climate models, will expand cropland suitability by an additional 16%, mainly in the Northern Hemisphere high latitudes. However, the tropics (mainly Africa, northern South America, Mexico and Central America and Oceania) will experience a small decrease in suitability due to climate change.

Main conclusions There is a large reserve of cultivable croplands, mainly in tropical South America and Africa. However, much of this land is under valuable forests or in protected areas. Furthermore, the tropical soils could potentially lose fertility very rapidly once the forest cover is removed. Regions that lie at the margins of temperature or precipitation limitation to cultivation are most sensitive to changes in climate and atmospheric CO_2 concentration. It is anticipated that climate change will result in an increase in cropland suitability in the Northern Hemisphere high latitudes (mainly in developed nations), while the tropics will lose suitability (mainly in developing nations).

Key words agricultural land, climate change, climate impact on cultivation, cropland, global, land suitability, land use.

INTRODUCTION

Since the emergence of agriculture almost 10 000 years ago, humans have derived a steady source of food supply from cultivation. Currently, about 12% of the land surface (18 million km^2, roughly the size of South America) is under some form of cultivation (Turner *et al.*, 1993; Ramankutty & Foley, 1998). However, a large part of the land surface is unsuitable for cultivation, due to limitations in growing season length, precipitation and soil moisture, soil characteristics or topography. Humans have overcome these limitations to some extent, through the use of irrigation and fertilization and terracing of the land surface.

Ultimately, crops are critically dependent on climate. They need an adequate growing season — warm temperatures for a sufficiently long time — for successful completion of all stages in their life cycle: germination, growth, floral initiation, grain filling and maturity. The boreal regions are normally too cold for cultivation, the temperate zones have sufficiently warm periods for many crops, while the tropics have adequately warm temperatures throughout the year (Cramer & Solomon, 1993; Leemans & Solomon, 1993). Crops are also dependent on an adequate supply of soil moisture. In fact, because the tropics have sufficiently warm temperatures throughout the year, cultivation is determined strongly by the distribution of

Correspondence: Navin Ramankutty; E-mail: nramanku@facstaff.wisc.edu

precipitation (Leemans & Solomon, 1993). Although irrigation has extended the boundaries of cultivation, several large regions of the world are still lacking cultivation because of the severe lack of water (e.g. the large subtropical deserts of Africa, Asia and Australia).

Soil properties are another major factor in cultivation. Soils with low organic content or acidic or highly alkaline soils are often unsuitable for cultivation. Organic matter greatly enhances, although indirectly, the quality of soils for plant productivity (Brady & Weil, 1996). Large regions of the tropics and subtropics have adequate temperature and moisture for cultivation. However, the warm temperatures result typically in greater microbial activity in the soil leading to smaller amounts of soil organic matter than in the temperate zones. Soil reaction (acidity, alkalinity or neutrality) influences many soil properties, including movement of air and water, breakdown of soil contaminants, plant nutrient availability and microbial activity (Brady & Weil, 1996). High rainfall intensity in the tropics and subtropics results in the leaching of base-forming cations, leading to soil acidity, while the opposite happens in low-rainfall regions, leading to alkalinity (Brady & Weil, 1996).

The relationships between climate and global plant distributions have been recognized for a long time (Holdridge, 1947; Box, 1981; Woodward & Williams, 1987). Larcher (1983) and Jones (1992) have described the climatic controls on plant physiological processes. In a similar fashion, several studies have tried to establish simple relationships between worldwide cropland distributions, climate and soil conditions. For example, Cramer & Solomon (1993) showed that the cold and dry boundaries of cultivated land could be quite adequately described using an index of growing season length and soil moisture availability to plants. Leemans & Solomon (1993) also examined the climatic limits to 10 major crops. However, both these studies developed a Boolean interpretation of land suitability for cultivation, i.e. each grid cell was considered to be entirely 'suitable for cultivation' or not at all. Also, the effects of soil characteristics were not adequately represented in these early studies.

Recently, there have been several advances that allow us to revisit this problem. With the use of remotely sensed data, consistent, globally gridded land cover classification datasets have been developed to provide an accurate picture of current cropland distributions. Furthermore, new global datasets of soil properties have emerged in recent years. In this study, we combine these new data with global climate data to derive a new assessment of global cropland suitability. Next, we evaluate the sensitivity of cultivable land to changes in temperature, precipitation, and atmospheric CO_2 concentrations. Finally, using four different climate model simulations, we examine the potential changes in cropland suitability due to climate change from increasing greenhouse gas concentrations, including the physiological effects of increasing CO_2 concentrations.

DATASETS

The International Geosphere–Biosphere Program, through its framework activity, Data and Information System (IGBP-DIS), has promoted the development of several global datasets, including a 1-km-resolution land-cover classification dataset (Loveland & Belward, 1997; Loveland *et al.*, 2000), and a 5-minute resolution (approximately 10 km on a side) global soil dataset (IGBP-DIS, 1998). With the availability of these high-resolution datasets, we can now define more accurately and precisely global land characteristics. In this study, we use these datasets to examine the relationships between cultivated land, climate variables and soil characteristics.

A continuous, globally consistent dataset of modern (*c.* 1992) croplands was developed recently by Ramankutty & Foley (1998). This dataset was created by calibrating the satellite-based IGBP-DIS 1-km land-cover classification dataset (Loveland *et al.*, 2000) against a worldwide collection of agricultural census data. The Ramankutty & Foley dataset was originally developed at a 5-minute by 5-minute latitude–longitude grid resolution, but we have aggregated it to a 0.5-degree resolution for this study. The dataset describes the fraction of each 0.5-degree grid cell occupied by cultivated land, wherein the definition of cultivated land follows that of the Food and Agricultural Organization (1995).

To derive the climatic limitations to crop growth, we use the newly developed CRU05 climatological dataset of New *et al.* (1999). This dataset represents the mean-monthly climate conditions for the 1961–90 period, and is provided in a gridded form with a resolution of 0.5 degrees latitude × longitude. The variables of interest used in this study are monthly temperature, precipitation and potential sunshine hours. To describe the soil limitations to cultivation, we use the recently developed IGBP-DIS (1998) global soil dataset, which contains various soil properties such as soil carbon density, soil nitrogen content, soil pH and soil water holding capacity, at a 5-minute resolution in both latitude and longitude. We further aggregated these data to a 0.5-degree resolution for this study.

MODEL DESCRIPTION

Previous studies have shown that the use of simple indices such as growing degree days (*GDD*) to represent growing season length and the ratio of actual evapotranspiration to potential evapotranspiration (α) to represent moisture availability to crops are sufficient to describe the cold and dry boundaries of agricultural land (Cramer & Solomon, 1993). In this study, we adopt these same indices as indicators of land suitability for cultivation, and estimate their spatial patterns using a very simple surface energy and water balance model (Prentice *et al.*, 1993; Foley, 1994; Haxeltine & Prentice, 1996).

The model is driven using the observed monthly mean climate data (surface air temperature, precipitation, and potential sunshine hours) of New *et al.* (1999). The monthly mean values are linearly interpolated to obtain daily mean values to drive the model. The model runs on a daily time step, except for the evapotranspiration calculations that run on a quasi-hourly time step (i.e. solar radiation, a component of evaporative demand is calculated on an hourly time step although the supply term is calculated daily).

GDD is calculated simply as an annual sum of daily mean temperatures over a base temperature of 5 °C, i.e.

$$GDD = \sum_{i=1}^{365} \max(0, T_i - 5) \text{ day-degrees.} \quad (1)$$

Net absorbed solar radiation, SW_{net}, is calculated as

$$SW_{net} = S_0(1-a)(c+dn)\cos(\xi)\ (\mathrm{W/m^2}), \quad (2)$$

where S_0 is the solar constant (1370 W/m^2), a is the average land surface albedo (0.17), c and d are constants (0.25 and 0.50, respectively), n is the fractional potential sunshine hours, and cos (ξ) is the cosine of the solar zenith angle. The net upward long-wave radiation, LW_{net}, is calculated as

$$LW_{net} = (b + (1-b)(1-n))(A - T)\ (\mathrm{W/m^2}), \quad (3)$$

where b and A are constants (0.2 and 107.0, respectively), and T is the air temperature (°C).

Equilibrium evapotranspiration (ET_{eq}) is a function of net radiation, and is calculated using the Penman equation:

$$ET_{eq} = \left(\frac{s}{s+\gamma}\right)\left(\frac{SW_{net} - LW_{net}}{L}\right)(\mathrm{mm/h}), \quad (4)$$

where s is the rate of change of saturated water-vapour pressure with respect to temperature, γ is the psychrometer constant (65 Pa/K) and L is the latent heat of vapourization of water (2.5×10^6 J/kg). SW_{net} is calculated on an hourly time step, while LW_{net} is calculated daily and assumed to be the same through the day.

Potential evapotranspiration (*PET*), or evaporative demand, is calculated following Monteith (1995) as:

$$PET = ET_{eq}\alpha_m[1 - \exp(-g_s/g_c)]\ (\mathrm{mm/h}), \quad (5)$$

where $\alpha_m = 1.26$ is the Priestley–Taylor coefficient (Priestley & Taylor, 1972), g_s is the canopy integrated stomatal conductance and g_c is a scaling conductance (chosen to be 0.2 mol/m^2 s^{-1} based on Monteith (1995). For present-day CO_2 concentrations, we estimate $g_s = 0.8$ mol/m^2 s^{-1} based on our coupled photosynthesis–stomatal conductance model, which is described later.

The actual supply of water, S, to meet this evaporative demand is simply calculated as:

$$S = ET_{\max}\frac{M}{M_{\max}}\ (\mathrm{mm/h}), \quad (6)$$

where $ET_{\max}$ is the maximum rate of evapotranspiration (1 mm/h), M is the daily soil moisture (mm) and $M_{\max}$ is the available water holding capacity (150 mm).

Actual evapotranspiration, ET_{act}, is the minimum of the evaporative demand and supply:

$$ET_{act} = \min(S, PET)(\mathrm{mm/h}), \quad (7)$$

Soil moisture is calculated using a simple bucket model:

$$\frac{dM}{dt} = P - ET_{act}\ (\mathrm{mm/day});\ M \le M_{\max}, \quad (8)$$

where P is the daily precipitation (mm/day). If $M > M_{\max}$, it is reset to $M_{\max}$, and the difference becomes runoff.

The availability of water to plants is expressed in terms of the moisture index:

$$\alpha = \frac{ET_{act}}{PET}. \quad (9)$$

In this study, we ran the model for 2 years to allow the soil moisture to come to equilibrium and used results from the second year. Figure 1 shows our simulated *GDD* and α.

INDEX OF LAND SUITABILITY FOR CULTIVATION

We develop an index of land suitability for cultivation that represents the probability that a particular grid cell will be cultivated. This index does not account for the productivity of a particular piece of land, but simply whether the characteristics of the land allow for cultivation. The index is continuous — each grid cell has a fractional value. We construct the index by examining existing relationships between croplands, climate indices, and soil characteristics indices.

We assume that land suitability for cultivation is a function of climate and soil properties. Other biophysical factors such as topography and irrigation, and socio-economic factors such as market price, incentive structure, etc. are obviously important for determining whether land will be cultivated. However, at the global scale, we find that climate and soil factors form the major constraints on cultivation, and adequately describe the major patterns of agricultural land as will be shown below. We choose growing degree days calculated on a 5-degree basis (*GDD*), and the ratio of actual *ET* to potential *ET* (α) as the indicators of climate suitability for cultivation (S_{clim}). Soil carbon density (C_{soil}) and soil pH (pH_{soil}) are chosen as the indicators of soil suitability for cultivation (S_{soil}).

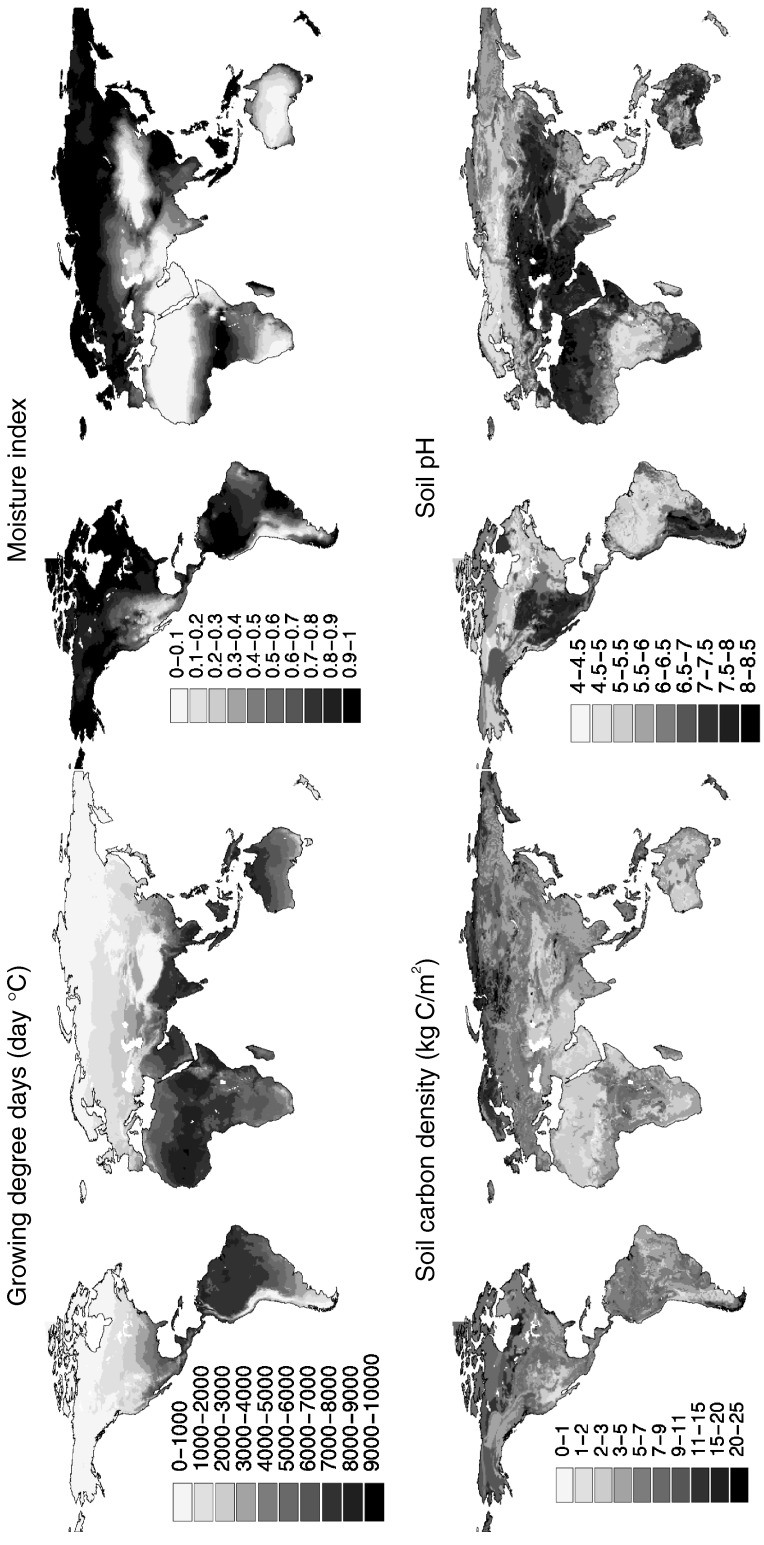

Fig. 1 Top panels: model simulated growing degree days (GDD) and moisture index. GDD is calculated as the annual sum of daily mean temperatures over a threshold of 5 °C. Moisture index is the ratio of actual evapotranspiration to potential evapotranspiration. Bottom panels: soil carbon density and soil pH in the top 30 cm of soil, from the IGBP-DIS dataset.

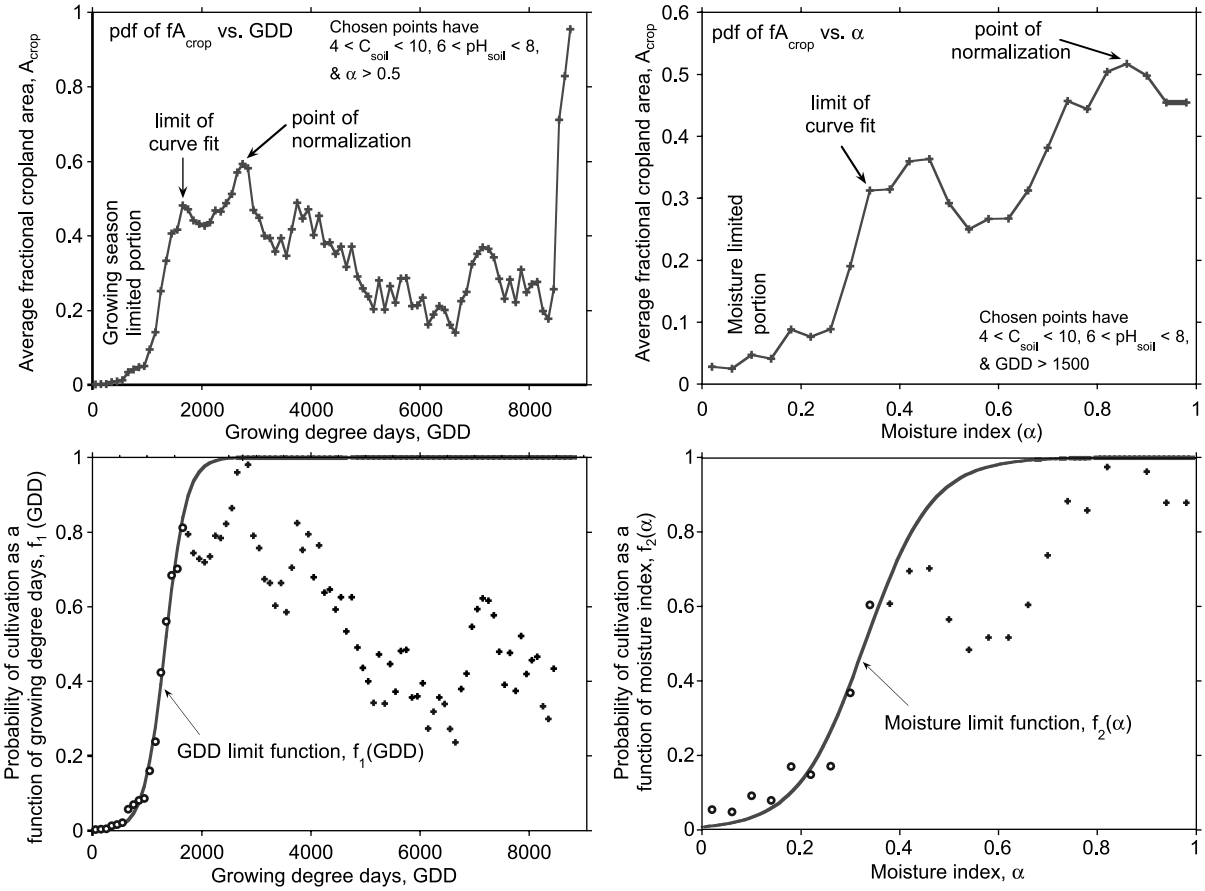

Fig. 2 Top panels: the probability density functions (pdf) of cropland area vs. growing degree days (*GDD*) and moisture index (α). The growing season and moisture limited portions of the curve are indicated. We normalize the probability density functions (pdfs) by the first peak in the relationship after which the cropland areas fall off (also indicated). Bottom panels: a sigmoidal curve has been fitted to the growing season and moisture limited portions of the normalized pdfs. In the top panels, we indicate the limiting point used in the curve fit. In the bottom panel, the open circles indicate points used in the curve fit.

Thus land suitability for cultivation, *S*, is given by,

$$S = S_{clim} \times S_{soil}, \tag{10}$$

where:

$$S_{clim} = f_1(GDD) f_2(\alpha), \tag{11}$$

and

$$S_{soil} = g_1(C_{soil})\, g_2(pH_{soil}). \tag{12}$$

In this study, we choose the suitability functions, $f_1(GDD)$, $f_2(\alpha)$, $g_1(C_{soil})$ and $g_2(pH_{soil})$, empirically, by fitting functions to the existing relationships between cropland areas, *GDD*, α, C_{soil}, and pH_{soil}.

We calculate the probability density function (pdf) of fractional cropland area, A_{crop}, vs. *GDD* and α (Fig. 2). Near the low end of *GDD* and α values, the growing season and moisture limitation to crops is evident. However, in the case of GDD, A_{crop} starts decreasing again after reaching a peak. This is because of two reasons: (1) regions with high *GDD* are also characterized by warm temperatures and high rainfall (i.e. the tropical areas), where the soil fertility is generally poor due to fast turnover of soil organic matter and rapid leaching of soil nutrients; and (2) these regions are currently occupied by tropical rain forests and were not exploited historically due to the difficulty in accessing them. Thus, we fit the *GDD* and α limited portions of the pdfs of A_{crop} by assuming a sigmoidal curve, after first normalizing by the value beyond which A_{crop} rapidly diminishes (Fig. 2). These sigmoidal functions define $f_1(GDD)$ and $f_2(\alpha)$, as:

$$f_1(GDD) = \frac{1}{\left[1 + e^{a(b-GDD)}\right]}, \tag{13}$$

and

$$f_2(\alpha) = \frac{1}{\left[1 + e^{c(d-\alpha)}\right]}, \quad (14)$$

where $a = 0.0052$, $b = 1334$, $c = 14.705$, and $d = 0.3295$.

The global patterns of soil carbon density and soil pH are shown in Fig. 1. These values are for the top 30 cm of soil, where crops have most of their roots. A small soil carbon density (a measure of the total organic content of the soil) does not provide sufficient nutrients for the crops, while a very large soil carbon density accumulates in the soil only if it is submerged under water (i.e. in wetlands). In the case of the latter, the soil has to be drained for cultivation, requiring an investment, and furthermore the soil carbon will be oxidized rapidly from a drained soil.

The pdf of A_{crop} vs. C_{soil} (Fig. 2) shows that there is an optimum range of C_{soil} in the range of 4–8 kg C/m^2. This lies in the Midwestern U.S. Corn Belt, the wheat–corn belt region of Eurasia, and the cultivated flood plains in India and China (see Fig. 1). These soil carbon density values are lower than would be expected of typical cultivated soils, but probably arise because the IGBP-DIS soil dataset represents the average value of a 0.5-degree resolution grid cell. However, as our relationships are empirically derived, we are not affected by this bias. We fit a double sigmoidal function to the relationship between A_{crop} and C_{soil}, and normalize the function to have a maximum value of 1.0 (lower panel of Fig. 2). This function is given by:

$$g_1(C_{soil}) = \frac{a}{\left[1 + e^{b(c-C_{soil})}\right]} \frac{a}{\left[1 + e^{d(e-C_{soil})}\right]}, \quad (15)$$

where $a = 3.9157$, $b = 1.3766$, $c = 3.468$, $d = -0.0791$, and $e = -27.33$.

Soil reaction (expressed as soil pH) influences suitability of land for cultivation because it influences nutrient availability. At pH < 5, eight of 13 essential nutrients become unavailable, and furthermore Al becomes more available and is highly toxic to plants. At pH > 8.5, nine of 13 essential nutrients become unavailable to plants (Brady & Weil, 1996). As a whole, a pH range of 6–7 seems to promote the best availability of nutrients to the majority of crops, although certain crops are adapted to more acidic or alkaline conditions. (We should note that there is considerable interest currently in genetically manipulating crops to make them capable of tolerating extreme levels of acidity or alkalinity.)

The pdf of A_{crop} vs. pH_{soil} (Fig. 3) shows that acidic soils have low cropland extent, and that there are very few samples of cropland area in alkaline soils. We choose a function with an optimum range of 6.5–8 based on that discussed in the foregoing paragraph (bottom panel of Fig. 3). We choose a linear fit through the portion of the A_{crop}–pH_{soil} relationship where A_{crop} is limited by acidity. However, Fig. 3 shows high cropland extent in alkaline soils, which is an artefact of the very few points actually sampled in alkaline soils. We choose a function that decreases linearly beyond a pH_{soil} of 8.0 to attain a value of zero at $pH_{soil} = 8.5$. Thus we have:

$$g_2(pH_{soil}) = \begin{cases} -2.085 + 0.475\ pH_{soil}, & if\ pH_{soil} \le 6.5 \\ 1.0, & if\ 6.5 < pH_{soil} < 8 \\ 1.0 - 2.0\ pH_{soil}, & if\ pH_{soil} \ge 8 \end{cases} \quad (16)$$

It is true that soils can normally be fertilized or treated to account for deficiencies in soil organic content or pH. However, such a treatment requires an investment and thus the suitability of this land is necessarily lower than land that requires no treatment. For example, the humid tropical soils of the Amazon or Congo river basin, dominated by Oxisols or Ultisols, are highly leached acidic soils low in nutrients. These soils could be managed for cultivation by applying lime and fertilizers, but this would be costly because these regions are far from sources of either lime or fertilizers.

From Fig. 4, we see that our estimate of S_{clim} captures the dry and cold boundaries of agriculture very well. Also, our estimate of S_{soil} shows clearly the highly fertile organic matter rich (chernozem) grassland soils (Mollisols) of the Midwestern United States, Ukraine, and the Pampas of Argentina. Our estimated index of land suitability for cultivation compares very well to our map of cropland area in 1992 (bottom panels of Fig. 4). Overall, the suitability index shows higher values than the current cropland map, which is realistic because many regions of the world with cultivation potential still remain uncultivated (Brady & Weil, 1996). Furthermore, in several regions of the world, alternative land use practices such as grazing/ranching or forestry are in competition with croplands for the same piece of land. Nevertheless, our suitability map represents the intensely cultivated regions such as the Corn Belt of the United States, the wheat–corn belt in the Former Soviet Union, and wheat-and-rice growing regions of China.

The largest area of remaining land with potential for cultivation is in South America and Africa. Much of this land is in forests or protected areas (Alexandratos, 1995). In South America, within the Amazon basin, this potential is currently being realized with the clearing of pristine tropical forests for pastures and croplands (Skole & Tucker, 1993; Moran *et al.*, 1994; Carvalho *et al.*, 2001). However, these tropical soils will not remain suitable for cultivation once the forest cover is removed. Tropical soils have low soil organic matter due to the rapid decomposition in warmer temperatures. Furthermore, the high rainfall rate leaches most of the valuable nutrients from the soil. The tropical forests are very successful at recycling nutrients. However, when the forest cover is removed and replaced with crops, the natural recycling of nutrients is lost (because crops are harvested and little organic matter reenters the soil), and the small quantities of organic matter and nutrients in the soil are quickly depleted (Brady & Weil, 1996).

The suitability map also shows greater potential for cultivation in Mexico and Central America, Argentina, north-east

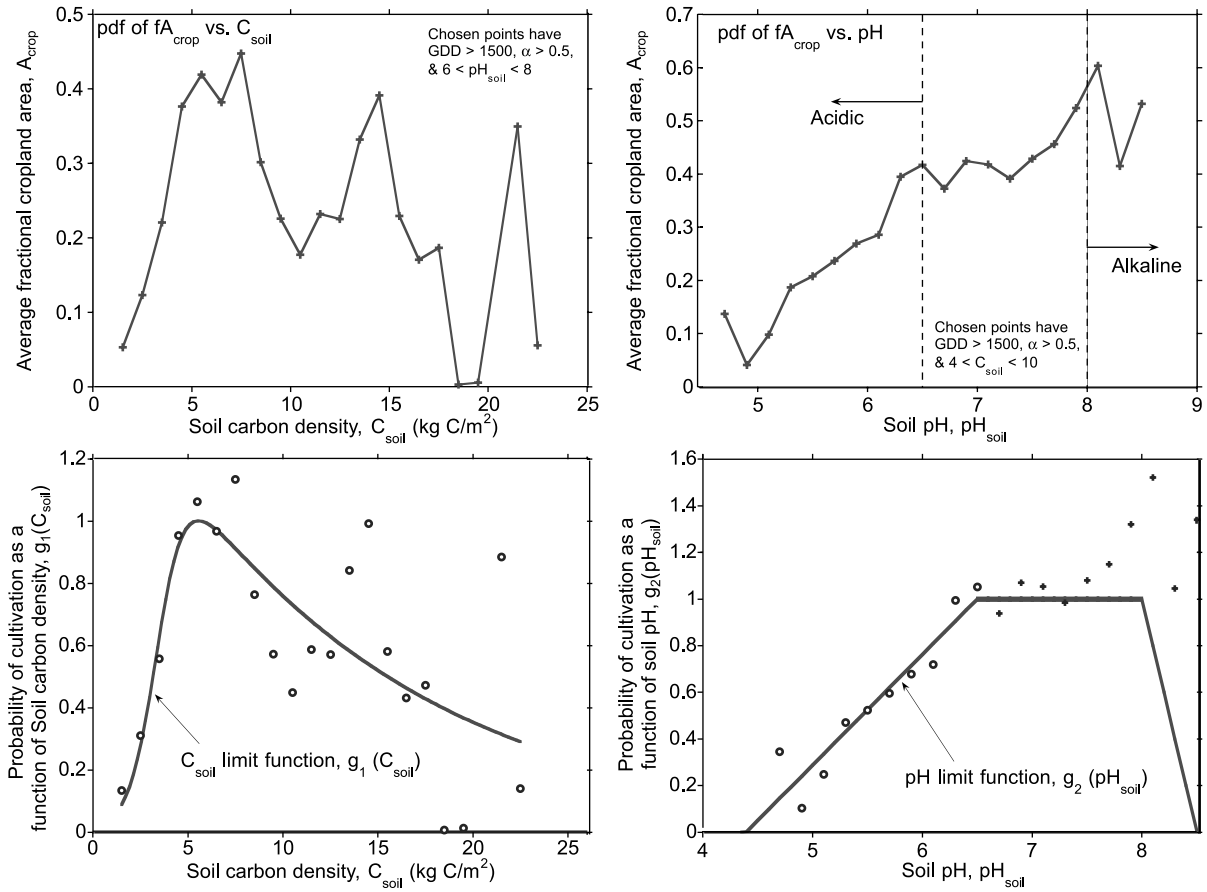

Fig. 3 The probability density functions (pdf) of cropland area vs. soil carbon density (C_{soil}) and soil pH (pH_{soil}) (top panels). Soil carbon density is closely associated with soil fertility for crops, and low values limit cultivation. High values of soil carbon density also limit cultivation because they are normally associated with wet soils that need to be drained before they can be cultivated. Soil pH limitations on cultivation are based on soils being too acidic or alkaline for cultivation. A double sigmoidal curve has been fitted to the cropland–soil carbon density relationship, and a combination of lines has been fitted to the cropland–pH relationship (lower panels).

China, South-east Asia and tropical Australia. The forests in South-east Asia are also being cleared currently and put to agricultural uses (Kummer & Turner, 1994). The suitability index underestimates the probability of cultivation in the Ganges flood plain, probably because this region has a long history of cultivation and is heavily irrigated (Döll & Siebert, 1999).

SENSITIVITY OF CROPLAND SUITABILITY TO CLIMATE CHANGE AND CHANGES IN ATMOSPHERIC CARBON DIOXIDE CONCENTRATION

There have been several previous studies evaluating the potential consequences of global climate change for food security (Rosenzweig & Parry, 1994; Parry *et al.*, 1999). These studies used point-level simulations of crop yields in several different parts of the world to examine how changes in climate might affect crop yields. Although these studies were valuable, they did not examine the potential shifts in locations of global agricultural land itself. Here, we examine the response of global cropland distribution to *any* change in climate, not just a particular global warming scenario. In particular, we test the sensitivity of the suitability index to changes in temperature and precipitation. This will allow us to identify which regions of the world are most sensitive to any potential changes in climate. Furthermore, we also evaluate the sensitivity of the suitability index to changes in atmospheric CO_2 concentration through its influence on stomatal physiology.

Sensitivity to climate change

We calculate the partial derivative of cropland suitability, S, with respect to temperature and precipitation as follows:

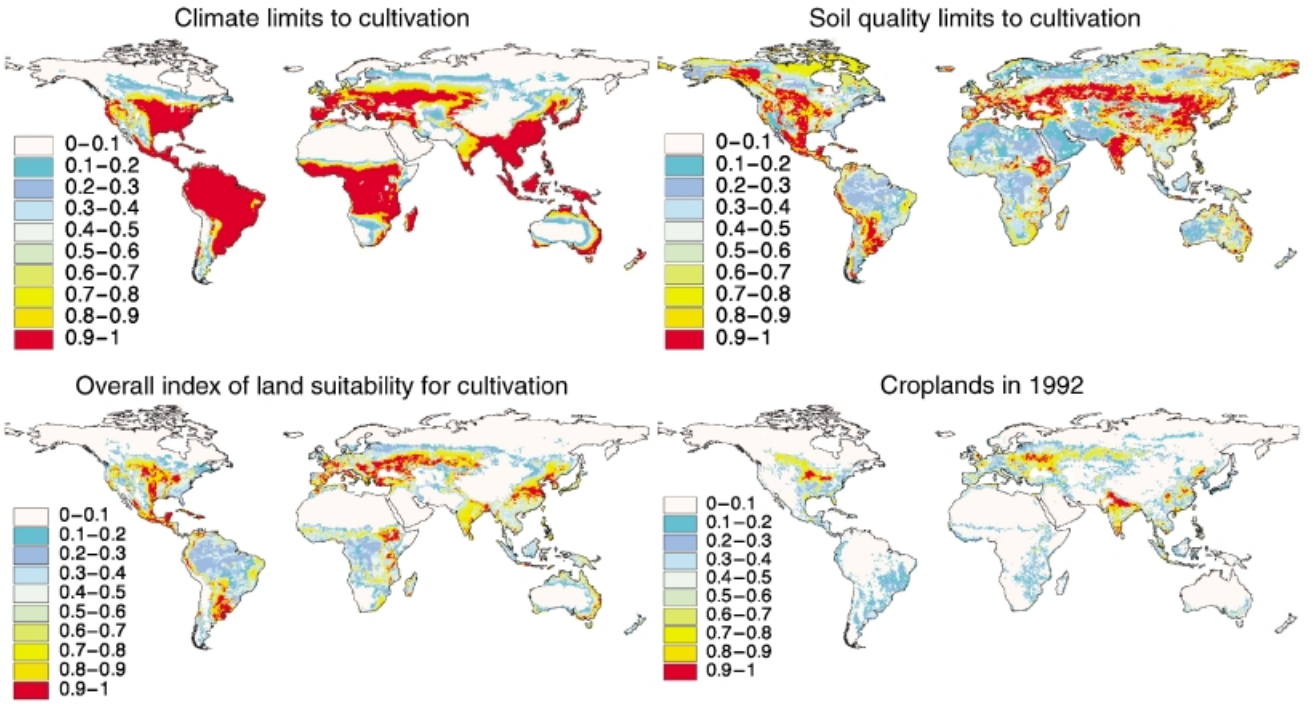

Fig. 4 Top panels: the climatic and soil quality limits to cultivation. The climatic limit is calculated by applying the GDD and moisture functions (Fig. 3) to their respective spatial data (Fig. 1). The soil quality limit is calculated by applying the soil carbon density and soil pH functions (Fig. 2) to their respective spatial data (Fig. 1). Bottom left panel: overall index of land suitability for cultivation derived as a product of the climate and soil quality limits to cultivation. Bottom right panel: the distribution of croplands in 1992, derived from Ramankutty & Foley (1998).

$S = f_1(GDD) f_2(\alpha) S_{soil}$.

We assume that S_{soil} is insensitive to changes in temperature and precipitation because the soil development process is slow. (This assumption might not be valid in some places where organic matter could build up relatively quickly. However this needs to be examined in detail in the future using a model of soil carbon dynamics.) We have:

$$\frac{\partial S}{\partial T} = S_{soil}\left(f_2(\alpha)\frac{\partial f_1(GDD)}{\partial T} + f_1(GDD)\frac{\partial f_2(\alpha)}{\partial T}\right), \quad (17)$$

and

$$\frac{\partial S}{\partial P} = S_{soil} f_1(GDD)\frac{\partial f_2(\alpha)}{\partial P}, \quad (18)$$

where T = local temperature and P = local precipitation.

This can be expanded further as:

$$\frac{\partial S}{\partial T} = S_{soil}\left(f_2(\alpha)\frac{\partial f_1(GDD)}{\partial GDD}\frac{\partial GDD}{\partial T} + f_1(GDD)\frac{\partial f_2(\alpha)}{\partial \alpha}\frac{\partial \alpha}{\partial T}\right), \quad (19)$$

and

$$\frac{\partial S}{\partial P} = S_{soil} f_1(GDD)\frac{\partial f_2(\alpha)}{\partial \alpha}\frac{\partial \alpha}{\partial P}. \quad (20)$$

From eqns 13 and 14, we have:

$$\frac{\partial f_1(GDD)}{\partial GDD} = \frac{a e^{a(b-GDD)}}{\left[1 + e^{a(b-GDD)}\right]^2}, \quad (21)$$

and

$$\frac{\partial f_2(\alpha)}{\partial \alpha} = \frac{c e^{c(d-\partial)}}{\left[1 + e^{c(d-\partial)}\right]^2}. \quad (22)$$

Thus all the terms in eqns 19 and 20 are known, except for $\frac{\partial GDD}{\partial T}$, $\frac{\partial \alpha}{\partial T}$, and $\frac{\partial \alpha}{\partial P}$. These additional terms cannot be calculated analytically. Thus, we estimate these terms by calculating their local derivative by perturbation experiments. We rerun the model described above by perturbing daily temperatures by +2.5 °C and –2.5 °C, and daily precipitation by +0.25 mm/day and –0.25 mm/day. These changes are roughly of the order of magnitude expected from a doubling of CO_2 concentrations (Houghton *et al.*, 1995). Let us denote the growing degree day values derived from the positive and negative temperature perturbation experiments as GDD_{T+} and GDD_{T-}, respectively, and the moisture index values as α_{T+} and α_{T-}, respectively. The moisture index values from the positive and negative precipitation perturbation experiments

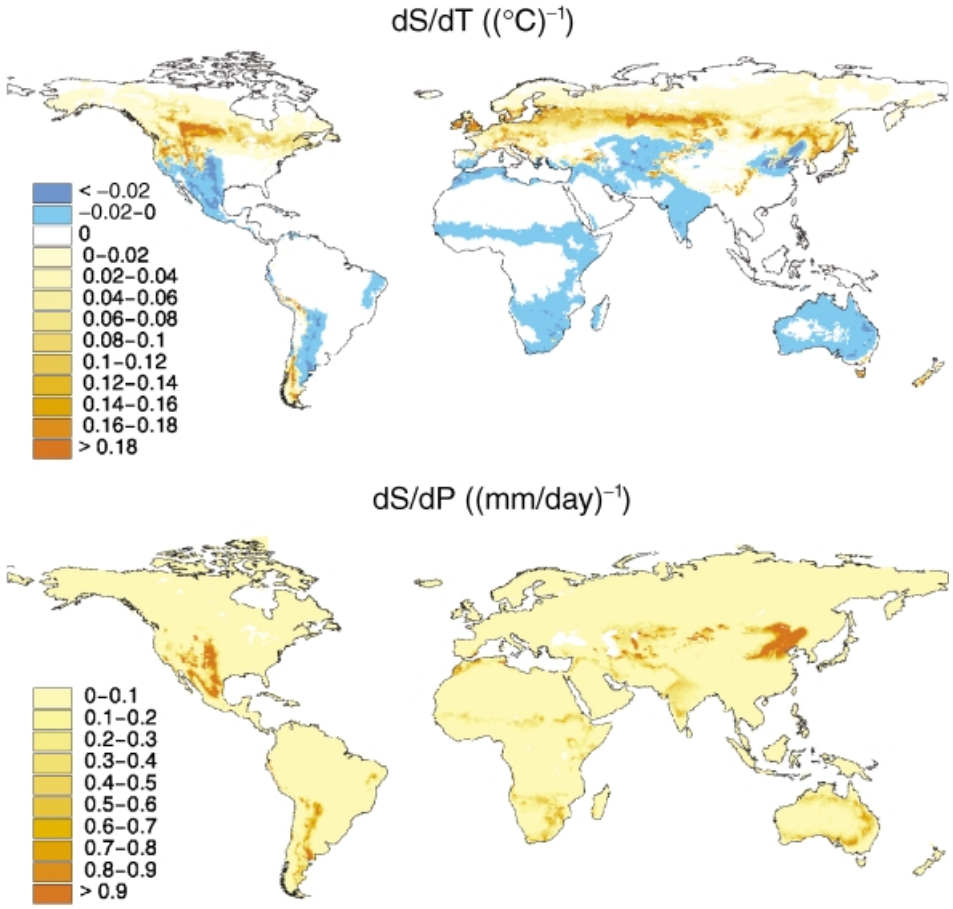

Fig. 5 The sensitivity of the index of cropland suitability to climate change. Partial derivative of cropland suitability index with respect to temperature (top panel) and precipitation (bottom panel). The regions lying at the margins of temperature and precipitation limitation to cultivation are most sensitive to changes in climate.

are denoted by α_{P+} and α_{P-}, respectively. Thus the local sensitivities of GDD and α to perturbations in temperature and precipitation can be calculated as:

$$\frac{\partial GDD}{\partial T} = \frac{GDD_{T+} - GDD_{T-}}{5.0}\text{days}, \quad (23)$$

$$\frac{\partial \alpha}{\partial T} = \frac{\alpha_{T+} - \alpha_{T-}}{5.0}\text{days}, \quad (24)$$

and

$$\frac{\partial \alpha}{\partial P} = \frac{\alpha_{P+} - \alpha_{P-}}{0.5}\text{days/mm}. \quad (25)$$

Figure 5 shows the sensitivity of the index of land suitability to changes in temperature and precipitation. In general, the suitability index shows the greatest sensitivity to change in those regions that are at the margins of cultivation. Indeed, the greatest sensitivities do occur in those regions where the slopes of the curves in Fig. 2 are highest, i.e. around a *GDD* of 1334, and α of 0.33. Too high or too low values of *GDD* and α will yield low sensitivities. High sensitivity to temperature is found in the southern provinces of Canada, the north-western and north-central states of the United States, northern Europe, southern Former Soviet Union, and the Manchurian plains of China. These regions lie at the margins of growing season limitation to cultivation (Figs 1 and 4). $\partial S/\partial T$ also has small negative values over large regions of the world that lie at the margins of moisture limitation to cultivation (Figs 1, 4 and 5). This is because of the increased evapotranspirational demand with increased temperatures.

The suitability index is very sensitive to changes in precipitation in the Great Plains region of the United States, and in north-eastern China. These are the regions that currently have agriculturally productive soils and sufficient growing season length, but are at the margins of moisture limitation for cultivation (Figs 1, 4 and 5). Large parts of India, western Argentina, north-east Brazil, subSaharan Africa, northern

and eastern borders of the Kalahari Desert, northern Kazakhstan, and northern and eastern Australia also show some sensitivity to precipitation.

Sensitivity to changes in atmospheric carbon dioxide concentrations

We calculate the partial derivative of cropland suitability, S, with respect to atmospheric carbon dioxide concentration, C, as follows:

$$\frac{\partial S}{\partial C} = S_{soil} f_1(GDD) \frac{\partial f_2(\alpha)}{\partial C} . \quad (26)$$

This can be expanded further as:

$$\frac{\partial S}{\partial C} = S_{soil} f_1(GDD) \frac{\partial f_2(\alpha)}{\partial \alpha} \frac{\partial \alpha}{\partial C} , \quad (27)$$

where $\frac{\partial f_2(\alpha)}{\partial \alpha}$ is given by eqn 22. All terms in eqn 27 are defined, except for $\frac{\partial \alpha}{\partial C}$. From eqns 7 and 9, we have:

$$\alpha = \frac{\min(S, PET)}{PET} . \quad (28)$$

This can be written as:

$$\alpha = \left\{ \begin{array}{l} \frac{S}{PET} \; if \; S < PET \\ 1 \; if \; S \geq PET \end{array} \right\} . \quad (29)$$

Thus, we have:

$$\frac{\partial \alpha}{\partial C} = \left\{ \begin{array}{l} \frac{-S \frac{\partial PET}{\partial C}}{PET^2} \; if \; S < PET \\ 0 \; if \; S \geq PET \end{array} \right\} . \quad (30)$$

From eqn 5, we have:

$$\frac{\partial PET}{\partial C} = \frac{ET_{eq} \alpha_m}{g_c} \exp(-g_s / g_c) \frac{\partial g_s}{\partial C} . \quad (31)$$

All the terms in eqns 30 and 31 are known, except for $\frac{\partial g_s}{\partial C}$. This last term represents the sensitivity of the canopy-integrated stomatal conductance to changes in atmospheric CO_2 concentration. To estimate this term, we run a coupled model of canopy photosynthesis and stomatal conductance. The leaf-level models for both C3 and C4 plants are based on the work of Collatz *et al.* (1991, 1992), and our implementation is described in Foley *et al.* (1996) and Kucharik *et al.* (2000). We scale the leaf-level values to the canopy level as a function of light extinction through the canopy, as described by Kucharik *et al.* (2000). Figure 6 (top panel) shows the simulation of canopy-integrated stomatal conductance as a function of ambient CO_2 concentration. For both C3 and C4 plants, the simulated canopy conductance decreases with increasing CO_2 as would be expected — plants close their stomata to conserve water because the increased gradient of CO_2 between the atmosphere and the intercellular air space allows them to achieve the same photosynthesis with a lower stomatal conductance. We average the results for C3 and C4 plants, fit a straight line to it between the average CO_2 concentration over the 1961–90 period (representative of the climate data) and 1000 p.p.m.v. (CO_2 concentrations are expected to rise in the future). The slope of the linear fit gives us an estimate of $\frac{\partial g_s}{\partial C}$.

Figure 6 shows the sensitivity of the index of land suitability to changes in atmospheric CO_2 concentration. The patterns of CO_2 sensitivity are similar to the patterns of precipitation sensitivity. This is reasonable because increased CO_2 makes more water available to plants due to stomatal closure, which is similar to increasing the precipitation. Thus, the regions of the world that are at the margins of precipitation are most sensitive to changes in ambient CO_2 concentrations. However, the magnitude of the change, even for a 100 p.p.m.v. change in CO_2 concentration used in this calculation, is very small compared to the sensitivity to changes in climate. This is because the influence of canopy conductance on PET is small until the conductance attains very small values (eqn 5) — as plants shut their stomata in response to increasing CO_2 while experiencing the same radiation regime, there is a switch toward dissipating that energy through evaporation rather than transpiration. Therefore total evapotranspiration remains high, until canopy conductance becomes very low, when PET decreases.

CHANGES IN CROPLAND SUITABILITY SUGGESTED BY GCM-SIMULATED CLIMATE CHANGE

In the earlier section, we explored the sensitivity of cropland suitability to arbitrary changes in temperature, precipitation and ambient CO_2 concentration. However, we performed the calculations by imposing uniform daily temperature or precipitation changes. Actual changes in climate expected from increasing greenhouse gas concentrations or sulphate aerosols are not likely to be uniform either seasonally or spatially. We therefore extend our study further to explore probable changes in suitability that might be expected from climate change due to increasing greenhouse gas concentrations as simulated by several climate models, as well as to anticipated changes in ambient CO_2 concentrations.

Several global climate models (GCMs) have been run in a transient mode using historical greenhouse gas concentrations, and into the future with projected greenhouse gas concentrations (Houghton *et al.*, 1995). Seven such simulations are

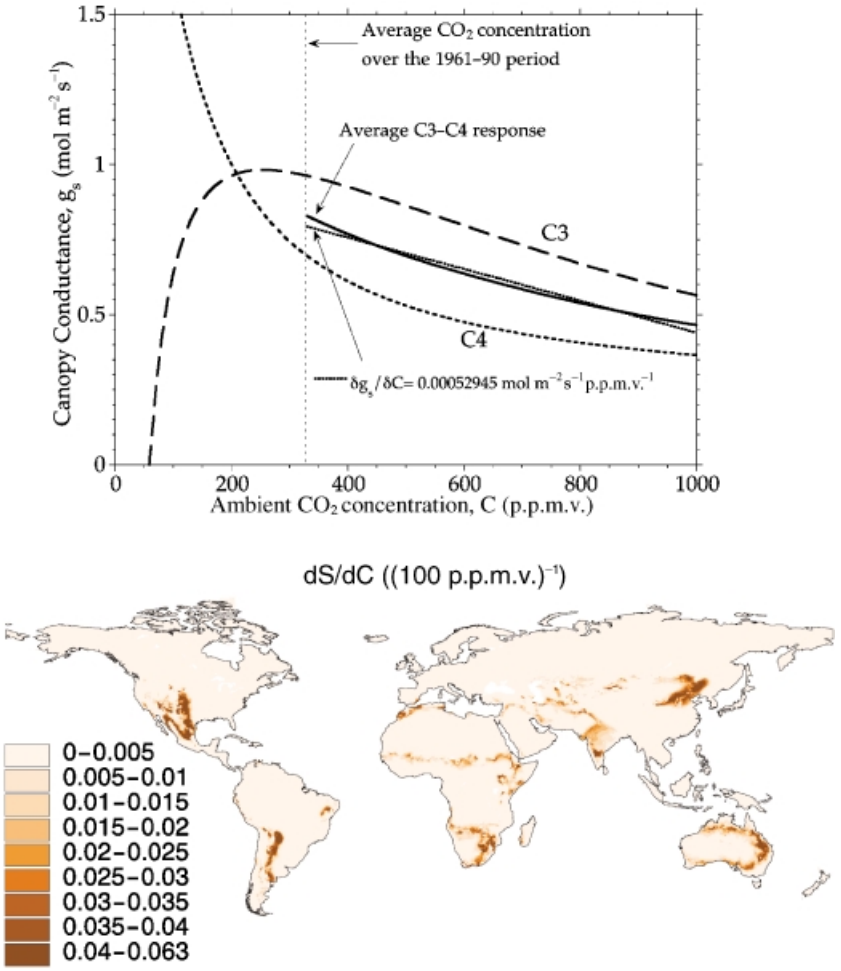

Fig. 6 Top panel: model simulation of the change in canopy conductance with ambient CO_2 concentration for C3 and C4 plants (see text for more detail on the model). The C3 and C4 response is averaged and a straight line fit to the response is chosen for use in our suitability study. Note that only CO_2 concentrations beyond the present-day value are used because we do not expect CO_2 to decrease in the near future. Bottom panel: the sensitivity of the index of cropland suitability to changes in ambient CO_2 concentrations. This is calculated as the partial derivative of cropland suitability index with respect to CO_2. The regions lying at the margins of precipitation limitation (Fig. 5, lower panel) are also the ones sensitive to CO_2. However, the magnitude of CO_2 sensitivity is much lower than that of climate sensitivity.

now archived in the IPCC Distributed Data Archive (http://ipcc-ddc.cru.uea.ac.uk/dkrz/dkrz_index.html). We pick four of the seven simulations for this study based on the criterion that they have run until 2100, using the IS92a 'business as usual' scenario of CO_2 concentrations (Houghton *et al.*, 1995) from 1990 to 2100 (or 1% annual increase of CO_2, which gives almost the same CO_2 concentrations). The chosen simulations are HADCM2 (from the Hadley Centre for Climate Prediction and Research, U.K.), ECHAM4 (from the Max-Planck-Institut für Meteorologie (MPI) and the Deutsches Klimarechenzentrum (DKRZ), Germany), CGCM (from the Canadian Center for Climate Modelling and Analysis) and CSIRO (from Australia's Commonwealth Scientific and Industrial Research Organization).

From the transient simulations, we retrieve monthly mean temperature and precipitation values, and calculate climatologies over the 1961–90 period and 2070–2099 period. The 1961–90 period represents the control because it covers the same period as the New *et al.* (1999) climate dataset, which we used to establish our land suitability index. The 2070–2099 climatology represents a changed climate scenario. The climate simulated by the GCMs for the 1961–90 period is reasonably similar to the observed datasets. Nevertheless, we avoid GCM biases in the present-day simulations by calculating the GCM simulated *changes* in climate from 1961–90 to 2070–99 and applying those changes to the observed 1961–90 climate to calculate an estimated climate for 2070–99. In particular, we calculate monthly mean climate change anomalies

for each GCM (difference anomalies are calculated for temperature, and proportional anomalies for precipitation). We then interpolate these anomalies from the GCM resolutions to a 0.5-degree resolution in latitude × longitude. We apply these anomalies to the New *et al.* (1999) climatological temperature and precipitation dataset (additive for temperature and multiplicative for precipitation) to obtain monthly mean temperature and precipitation scenarios for the 2070–99 period as simulated by four GCMs (the resulting precipitation is bound between 0 and 200 mm/month). For the 2070–99 period, the ambient CO_2 concentration is 710 p.p.m.v., for which our simulated canopy conductance is 0.58 mol/m^2 s^{-1}. This change in ambient CO_2 concentration will cause only a 3.3% decrease in PET. Of course, a caveat to be mentioned is that we are not including the effects of ambient CO_2 concentration on productivity.

We now rerun our simple water balance model and growing degree day calculations for the changed climate scenarios and modified canopy conductance, and calculate, using eqns 1–16, land suitability for agriculture expected in the 2070–99 period, due to climate change. We then calculate the average results from the four GCMs, of the change in suitability in 2070–99 compared to our 1961–90 base (Fig. 7). We average the GCM results only if at least three of the four GCMs agree in the sign of the change; if any two GCMs show a change in suitability in opposite direction from the other two, we assume that there is no change in suitability.

One of the most common responses of GCMs to increasing greenhouse gas concentrations is an enhanced warming of the high latitudes owing to sea-ice feedback. Coupling this climate response to the fact that the Northern Hemisphere high latitude regions are growing season limited results in an overwhelming response of increased suitability in Canada, northern Europe, Siberia, Mongolia, and northern China due to climate change. The mountainous regions of the world, in the Andes, and in the Himalayas, show some increase in suitability owing to an increase in growing season. The high-latitude Southern Hemisphere regions — southern tip of Argentina and Chile, Tasmania, and New Zealand — also show increases in suitability. The rest of the world, especially those regions at the margins of moisture limitation, shows a slight decrease in suitability owing to increased ET demand associated with increased temperatures. Again, we would like to emphasize that this represents only the changes in probability that land will be cultivated, irrespective of the actual changes in yield of land that might result from climate change.

DISCUSSION AND CONCLUSIONS

We have shown that a reasonable global map of land suitability for cultivation can be constructed using a few carefully chosen climate indices and soil parameters. The total global extent of suitable cropland in the current climate is 41 million km^2. This is roughly 120% larger than the 1992 global cropland area of 18 million km^2.

The greatest potential for croplands in the current climate exists in Tropical Africa (5.6 million km^2) and northern South America (4.7 million km^2) according to our regional calculations (Fig. 8). This result is not entirely new; previous studies have also identified these regions as being the cropland reserves (Buringh & Dudal, 1987; Alexandratos, 1995). Indeed, the tropical forests and woodlands are just beginning to be exploited. The forests in Amazonia are being cleared at a rapid rate for ranching (Skole *et al.*, 1994). Brazil is the second largest producer of soybeans (Brown, Renner & Halwell, 2000; Sebastian & Wood, 2000), and it is anticipated that continued paving of highways in Amazonia will continue, justified by savings in transportation costs to soy producers (Carvalho *et al.*, 2001). However, as discussed earlier, tropical soils will lose fertility rapidly once the forest cover is replaced with a crop, and will require expensive inputs to maintain the soil nutrients and conserve soil organic matter. In fact, Sebastian & Wood (2000) find that the nutrient balance for most crops and cropping systems in Latin America and the Caribbean is significantly negative.

In South Asia, we estimate less suitable cropland than is actually cultivated. Comparison of the maps of suitable and actual cropland area in Fig. 4 shows that this lies mainly in the Ganges flood plain region. This region has a long history of agriculture, and is heavily irrigated (Döll & Siebert, 1999). In the future, our study needs to be extended to account for the influence of irrigation water availability on cropland suitability.

From our sensitivity analysis, we find that the southern provinces of Canada, north-western and north-central states of the United States, northern Europe, southern former Soviet Union, and the Manchurian plains of China are most sensitive to changes in temperature. The Great Plains region of the United States and north-eastern China are most sensitive to changes in precipitation.

In the GCM-simulated climate of 2070–99, we estimate an increase in suitable cropland area of 6.6 million km^2 (an increase of roughly 16%). Most of this increase comes from the high latitude regions: former Soviet Union (3.4 million km^2), Canada (1.5 million km^2), and China, Mongolia, & North Korea (0.9 million km^2). The tropical regions (Africa, northern South America, Mexico and Central America, and Oceania) have a small decrease in suitability. Such potential changes in cropland suitability due to climate change will further enhance the food-security divide between the developed countries of the Northern Hemisphere high latitudes and the developing countries of the tropics.

Our index of land suitability for cultivation is simply a measure of the probability that land will be cultivated. It does not quantify exactly the ultimate productivity of the land, which is largely controlled by local management decisions.

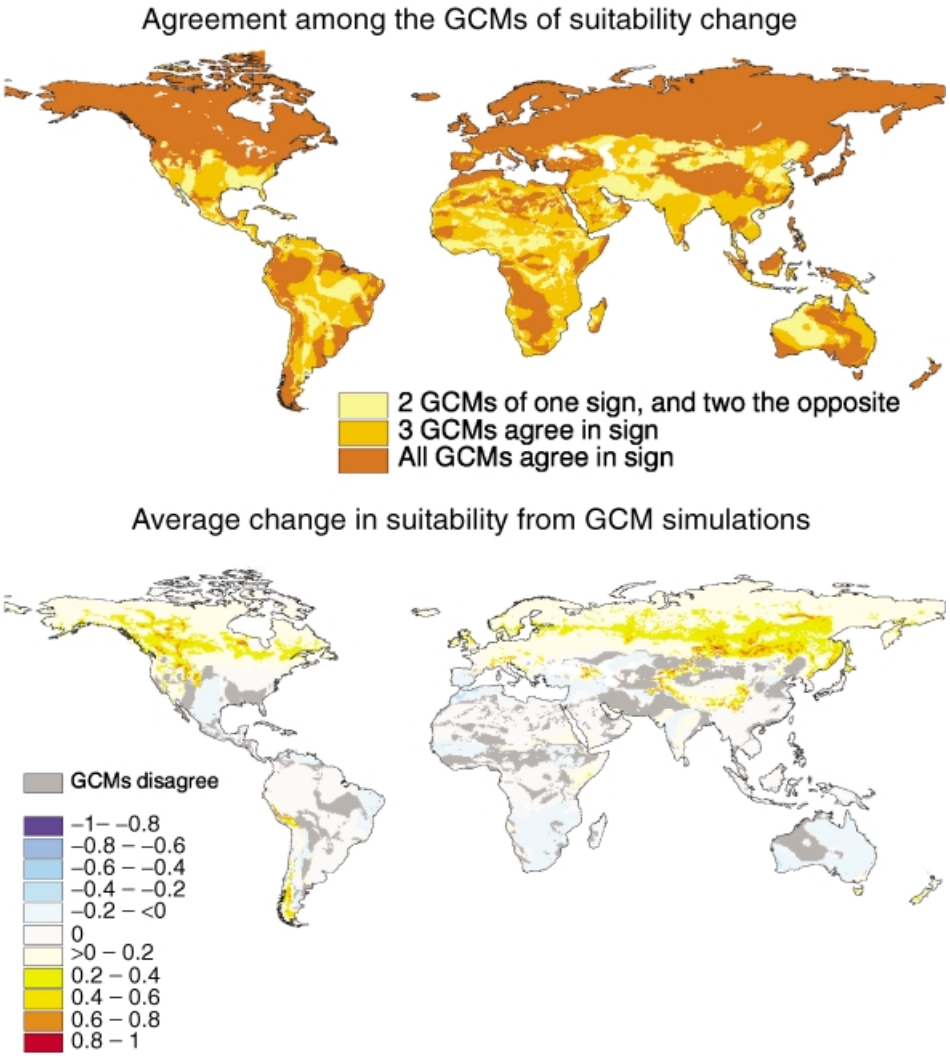

Fig. 7 Change in global cropland suitability with climate change. We used the simulations from four different global climate models run with increasing greenhouse gas concentrations ('business as usual' scenario) into the 21st century. Here we analyse the influence on cropland suitability, of simulated climate change in 2070–99 compared to the 1961–90 period. Top panel: map of agreement among the GCMs of the direction of change in cropland suitability due to climate change. Bottom panel: average change in suitability estimated by the GCMs, if at least three GCMs agree. The GCMs simulations imply that climate change will cause cropland suitability to increase in the Northern Hemisphere high latitudes and decrease in the tropics.

Although global climate change due to increasing greenhouse gases might increase the area of land that is cultivable, the actual yield of crops might decrease. Thus, in the future, this estimate needs to be improved by including a measure of crop productivity. Furthermore, the effects of climate change on soil properties need to be accounted for. We could incorporate additional soil properties such as soil nitrogen density and soil texture. The ratio of soil mineral content to soil organic matter could be used to evaluate the rate at which soil organic carbon might be oxidized upon being drained. A soil with a high percentage of clay mineral content will bind the organic matter to the mineral particles, lowering the oxidation rates.

Currently, our index is derived empirically by examining existing relationships between current cropland area, climate and soil characteristics. These relationships may not remain valid in a different future climate. However, our sensitivity analysis still remains valid, because it is based on analysis of perturbations around the current climate. Future improvements should include more mechanistic representations of

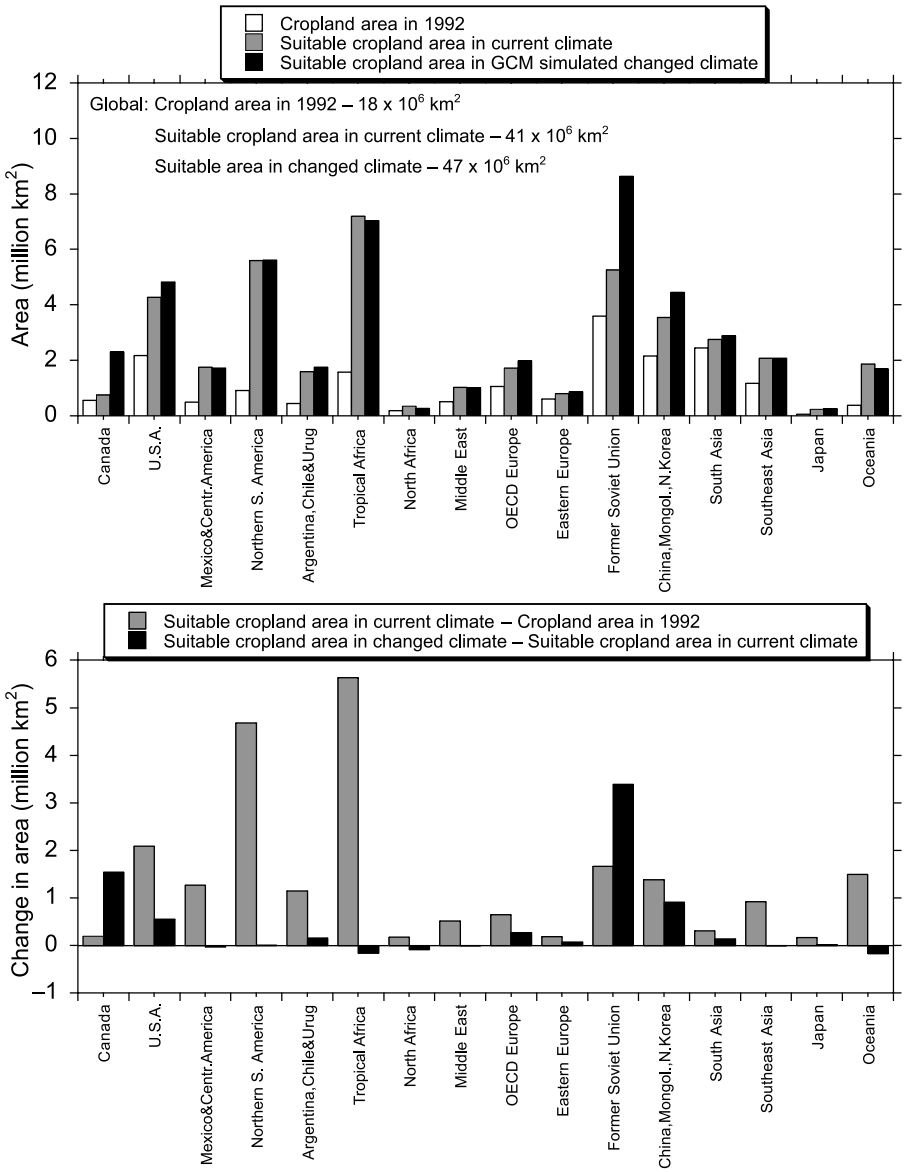

Fig. 8 Top panel: regional averages of current cropland area, suitable cropland area under current climate, and suitable cropland area in a GCM-simulated climate for the 2070–99 period. Bottom panel: differences in areas shown on the top panel indicating the additional potential for cultivation under current climate, and the change in this potential in the event of climate change.

soil characteristics and climate parameters. Also, the loss of land suitability due to soil erosion, accelerated acidification, and salinization could be incorporated. The influences of topography and irrigation need to be included. Finally, the competition between different sectors of the economy, such as forestry, urbanization, etc. for the same piece of land has to be accounted for. For instance, a large area of prime farmland in the United States and China is currently being lost to urbanization (Gardner, 1996; Sorensen *et al.*, 1997; Heilig, 1999).

ACKNOWLEDGMENTS

We would like to thank Mike Coe for useful discussions on this paper. This work was supported by NASA's Office of Earth Science (through an Interdisciplinary Science Investigation)

and by a NASA Earth System Science Fellowship to Navin Ramankutty.

REFERENCES

Alexandratos, N., ed. (1995) *World agriculture towards 2010*. Food and Agriculture Organization of the United Nations, Rome.

Box, E.O. (1981) *Macroclimate and plant forms: an introduction to predictive modeling in phytogeography*. Dr W. Junk Publishers, Berlin.

Brady, N.C. & Weil, R.R. (1996) *The Nature and Properties of Soils*. Prentice Hall, New Jersey.

Brown, L.R., Renner, M. & Halwell, B. (2000) *Vital signs 2000: the environmental trends that are shaping our future*. W.W. Norton Co., New York.

Buringh, P. & Dudal, R. (1987) Agricultural land use in space and time. *Land transformation in agriculture* (ed. by M.G. Wolman and F.G.A. Fournier), pp. 3–43. John Wiley & Sons, Chichester.

Carvalho, G., Barros, A.C., Moutinho, P. & Nepstad, D. (2001) Sensitive development could protect Amazonia instead of destroying it. *Nature*, **409**, 131–131.

Collatz, G.J., Ball, J.T., Grivet, C. & Berry, J.A. (1991) Physiological and environmental regulation of stomatal conductance, photosynthesis and transpiration: a model that includes a laminar boundary layer. *Agricultural and Forest Meteorology*, **53**, 107–136.

Collatz, G.J., Ribas-Carbo, M. & Berry, J.A. (1992) Coupled photosynthesis–stomatal conductance model for leaves of C_4 plants. *Australian Journal of Plant Physiology*, **19**, 519–538.

Cramer, W.P. & Solomon, A.M. (1993) Climatic classification and future global redistribution of agricultural land. *Climate Research*, **3**, 97–110.

Döll, P. & Siebert, S. (1999) *A digital global map of irrigated areas: Documentation*. Report no. A9901. Center for Environmental Systems Research, University of Kassel, Kassel. http://www.usf.uni-kassel.de.

Foley, J.A. (1994) Net primary productivity in the terrestrial biosphere: the application of a global model. *Journal of Geophysical Research*, **99**, 20773–20783.

Foley, J.A., Prentice, C.I., Ramankutty, N., Levis, S., Pollard, D., Sitch, S. & Haxeltine, A. (1996) An integrated biosphere model of land surface processes, terrestrial carbon balance, and vegetation dynamics. *Global Biogeochemical Cycles*, **10**, 603–628.

Food and Agriculture Organization (1995) *Land use, FAOSTAT-PC*. Food and Agriculture Organization of the Uited Nations, Rome.

Gardner, G. (1996) *Shrinking fields: cropland loss in a world of 8 billion*. Report no. Worldwatch Paper 131. Worldwatch Institute, Washington, DC.

Haxeltine, A. & Prentice, C.I. (1996) BIOME3: an equilibrium terrestrial biosphere model based on ecophysiological constraints, resource availability, and competition among plant functional types. *Global Biogeochemical Cycles*, **10**, 693–709.

Heilig, G.K. (1999) *Can China feed itself? — a system for evaluation of policy options*. International Institute for Applied Systems Analysis, http://www.iiasa.ac.at/Research/LUC/ChinaFood/index_m.htm.

Holdridge, L.R. (1947) Determination of world plant formations from simple climatic data. *Science*, **105**, 367–368.

Houghton, J.T., Filho, L.G.M., Callander, B.A., Harris, N., Kattenberg, A. & Maskell, K., eds (1995) *Climate change 1995: the science of climate change*. Cambridge University Press, Cambridge.

IGBP-DIS (1998) *Soildata (V 0): a program for creating global soil-property databases*. IGBP Global Soils Data Task, France.

Jones, H.G. (1992) *Plants and microclimate: a quantitative approach to environmental plant physiology*, 2nd edn. Cambridge University Press, Cambridge.

Kucharik, C.J., Foley, J.A., Delire, C., Fisher, V.A., Coe, M.T., Lenters, J.D., Young-Molling, C., Ramankutty, N., Norman, J.M. & Gower, S.T. (2000) Testing the performance of a Dynamic Global Ecosystem Model: water balance, carbon balance, and vegetation structure. *Global Biogoechemical Cycles*, **14**, 795–825.

Kummer, D.M., Turner, B.L. & I.I. (1994) The human causes of deforestation in southeast asia. *Bioscience*, **44**, 323–328.

Larcher, W. (1983) *Physiological plant ecology*, 2nd edn. Springer-Verlag, New York.

Leemans, R. & Solomon, A.M. (1993) Modeling the potential change in yield and distribution of the Earth's crops under a warmed climate. *Climate Research*, **3**, 79–96.

Loveland, T.R. & Belward, A.S. (1997) The IGBP-DIS global 1 km land cover dataset, DISCover: first results. *International Journal of Remote Sensing*, **18**, 3289–3295.

Loveland, T.R., Reed, B.C., Brown, J.F., Ohlen, D.O., Zhu, J., Yang, L. & Merchant, J.W. (2000) Development of a global land cover characteristics database and IGBP DISCover from 1-km AVHRR Data. *International Journal of Remote Sensing*, **21**, 1303–1330.

Monteith, J.L. (1995) Accommodation between transpiring vegetation and the convective boundary layer. *Journal of Hyrology*, **166**, 251–263.

Moran, E.F., Brondizio, E., Mausel, P. & Wu, Y. (1994) Integrating amazonian vegetation, land-use, and satellite data. *Bioscience*, **44**, 329–338.

New, M.G., Hulme, M. & Jones, P.D. (1999) Representing twentieth-century space–time climate variability. Part I: Development of a 1961–90 mean monthly terrestrial climatology. *Journal of Climate*, **12**, 829–856.

Parry, M., Rosenzweig, C., Iglesias, A., Fischer, G. & Livermore, M. (1999) Climate change and world food security: a new assessment. *Global Environmental Change-Human and Policy Dimensions*, **9**, S51–S67.

Prentice, I.C., Sykes, M.T. & Cramer, W. (1993) A simulation model for the transient effects of climate change on forest landscapes. *Ecological Modeling*, **65**, 51–70.

Priestley, C.H.B. & Taylor, R.J. (1972) On the assessment of surface heat flux and evaporation using large-scale parameters. *Monthly Weather Review*, **100**, 81–92.

Ramankutty, N. & Foley, J.A. (1998) Characterizing patterns of global land use: an analysis of global croplands data. *Global Biogeochemical Cycles*, **12**, 667–685.

Rosenzweig, C. & Parry, M.L. (1994) Potential impact of climate change on world food supply. *Nature*, **367**, 133–137.

Sebastian, K.L. & Wood, S. (2000) *Spatial aspects of evaluating technical change in agriculture in Latin America and the Caribbean (LAC)*. International Food Policy Research Institute, Washington, D.C.

Skole, D.L., Chomentowski, W.H., Salas, W.A. & Nobre, A.D. (1994) Physical and human dimensions of deforestation in Amazonia. *Bioscience*, **44**, 314–322.

Skole, D. & Tucker, C. (1993) Tropical deforestation and habitat fragmentation in the Amazon: satellite data from 1978 to 1988. *Science*, **260**, 1905–1910.

Sorensen, A.A., Greene, R.P. & Russ, K. (1997) *Farming on the edge*. American Farmland Trust, Center for Agriculture in the Environment, Northern Illinois University, DeKalb, Illinois (http://www.farmlandinfo.org/cae/foe2/foetoc.html).

Turner II, B.L., Moss, R.H. & Skole, D.L. (1993) *Relating land use and global land-cover change: a proposal for an IGBP-HDP core project*. IGBP report no. 24, HDP report no. 5, 65. International Biosphere–Geosphere Program: a study of global change and the human dimensions of global environmental change programme, Stockholm.

Woodward, F.I. & Williams, B.G. (1987) Climate and plant distribution at global and local scales. *Vegetatio*, **69**, 189–197.

BIOSKETCHES

Navin Ramankutty is a research scientist at the Center for Sustainability and the Global Environment (SAGE) at the University of Wisconsin. His research interest is in understanding the ecosystem consequences of human activities.

Jon Foley is the director of SAGE and associate professor in the Institute for Environmental Studies at the University of Wisconsin. His work focuses on the dynamics of global environmental systems, and their interactions with human societies.

John Norman is a professor in soil science at the University of Wisconsin. He studies the interactions between various components of the soil–plant–atmosphere–animal system with the use of numerical models and field observations.

Kevin McSweeney is associate dean of the school of natural resources and professor in soil science at the University of Wisconsin. He studies the nature, function and distribution of soils on the landscape and applies this knowledge to develop strategies that foster sustainable land management.